引用格式：ZHAO Dechun, SONG Yansong, LIU Yang, et al. Sliding Mode Control of Tip-tilt Mirror Based on Disturbance Observer[J]. Acta Photonica Sinica, 2022, 51(6):0601002
赵德春,宋延嵩,刘洋,等.基于扰动观测器的倾斜镜滑模控制[J].光子学报,2022,51(6):0601002

基于扰动观测器的倾斜镜滑模控制

赵德春[1],宋延嵩[2,3],刘洋[2,3],董岩[1,2],张柏硕[3]
(1 长春理工大学 电子信息工程学院,长春 130022)
(2 长春理工大学 空地激光通信国防重点学科实验室,长春 130022)
(3 长春理工大学 光电工程学院,长春 130022)

摘 要:为解决在外部扰动情况下自适应光学中倾斜镜的控制问题,提出了一种基于扰动观测器的滑模控制方法来抑制结构振动。在倾斜镜控制系统中,将新的扰动观测器加入到传统滑模控制方法中,设计新的滑模控制率来抑制抖振。改进后的扰动观测器不受精确模型的限制,仿真结果证明了该方法能够比较准确的跟踪系统状态,抑制扰动效果明显,降低了系统误差,输出曲线更接近给定的输入信号。实验结果表明,所设计的方法与传统滑模控制方法相比,方位轴控制误差由1.637 μrad降低到1.083 μrad,精度提高约51.2%,俯仰轴控制误差由1.966 μrad降低到1.614 μrad,精度提高约21.8%。该方法可大幅削弱由滑模控制方法造成的抖振及外部扰动,提高倾斜镜控制系统的稳定性。

关键词:自适应光学;倾斜镜;滑模控制;扰动观测器;抖振
中图分类号:TP273.2 **文献标识码**:A **doi**:10.3788/gzxb20225106.0601002

0 引言

在无线激光通信系统中,自适应光学系统中倾斜镜被广泛应用,能够实时校正光束偏移、稳定对准接收端[1],具有运动惯性小[2]、响应速度快、角分辨精度高、抗电磁干扰能力强等显著优点。由大气湍流引起的整体倾斜约占扰动误差的87%[3],因此,倾斜镜系统对于校正一阶倾斜起到至关重要的作用。

自适应光学系统中倾斜镜由于受到风振,设备振动和平台振动,严重影响了系统的闭环性能[4-5],因此,为了达到光学的衍射极限,必须减轻振动。传统的闭环反馈控制对倾斜镜振动的抑制能力较差,导致闭环性能降低,因此,研究新的抗振技术对提高倾斜镜闭环性能至关重要。目前,已经有很多种抑制振动的方法,例如:文献[6-7]提出一种基于扰动的前馈控制对倾斜镜系统结构振动的抑制方法,该控制器可以产生高抑制带宽,因此不受低速率采样的限制,然而加速度计或者陀螺仪[8]的低频漂移和高频噪声严重影响了振动的估计精度。由于现有的控制系统带来了额外的控制问题,许多研究人员专注于设计先进的控制器来抑制振动。在积分控制器的前提下,提出了线性二次高斯控制器和H_∞/H_2控制器[9-10]来提高倾斜镜在振动下的闭环性能。然而,闭环系统的性能取决于控制对象的模型精度和振动,尤其是在倾斜镜控制系统中,如果存在较大的模型误差,会使系统性能大大降低。由于干扰通常发生在低频域[11-13],而传感器噪声发生在高频域,因此在能够准确估计或测量干扰的情况下,采用扰动观测器对低频域的干扰进行抑制。在许多伺服控制系统中[14-16],Q31-滤波器通常被用作最优滤波器,在控制带宽和鲁棒稳定性方面对闭环性能进行优化,然而在低频和中频干扰较大时,则需要低通滤波器的高带宽。滑模控制(Sliding Mode Control, SMC)因其算法简单,具有强大的抗干扰能力和克服系统不确定性的能力,被广泛应用到工业中。然而,许多实际系统中存在的不确定性不满足系统的匹配条件。例如:由于参数变化和负载转矩造成的不确定性的永磁同步电机

基金项目:吉林省科技厅自然科学基金(No. YDZJ202101ZYTS193)
第一作者:赵德春(1996—),男,硕士研究生,主要研究方向为自动控制及伺服控制等。Email:1298083629@qq.com
导师(通讯作者):宋延嵩(1983—),男,副研究员,博士,主要研究方向为空间激光通信系统光束伺服、光电跟踪和光电测试等。Email:songyansong2006@126.com
收稿日期:2022-01-06;**录用日期**:2022-01-27

系统[17]，未对动力学建模、外部风振和参数变化引起集中扰动转矩的飞行控制系统[18]，对于这些系统，传统SMC的滑模运动会受到不匹配扰动的影响，使其鲁棒性能大大降低。

本文提出一种新的SMC方法，通过扰动观测器（Disturbance Observer，DOB）来抑制系统中的振动，设计一种新的基于扰动估计的滑模面，即使存在不匹配扰动的情况下，也能通过滑模面使系统状态渐进地达到理想的平衡状态。然后，设计了带有高频切换增益的不连续控制率，迫使系统初始状态到达所设计的滑模面。该方法的主要优点有：1）所提出的控制率中的高频切换增益只需要设计大于扰动估计误差的边界，而不需要设计大于扰动的边界，从而大大缓解了抖振问题；2）在不存在不确定性扰动的情况下，不会对系统造成不利影响。

1 传统滑模控制（SMC）方法

对于存在未知外部扰动的二阶系统，可表示为

$$\begin{cases}\dfrac{\mathrm{d}x_1}{\mathrm{d}t}=x_2+d(t)\\ \dfrac{\mathrm{d}x_2}{\mathrm{d}t}=a(x)+b(x)u\\ y=x_1\end{cases}\tag{1}$$

式中，x_1和x_2分别为系统的状态量，$a(x)$为系统状态多项式，$b(x)$为带有系统状态的输入多项式，u为系统的输入，$d(t)$为外部扰动，y为系统的输出。传统的滑模面和控制率设计为

$$\begin{aligned}&s=x_2+cx_1\\&u=-b^{-1}(x)\left[a(x)+cx_2+k\,\mathrm{sgn}(s)\right]\end{aligned}\tag{2}$$

将式（1）代入式（2）可得

$$\frac{\mathrm{d}s}{\mathrm{d}t}=-k\,\mathrm{sgn}(s)+cd(t)\tag{3}$$

假设1：系统（1）中的扰动有界，且满足$d^*=\sup\limits_{t>0}\left|d(t)\right|$。$\sup|\cdot|$为函数的上确界。

从式（3）中可以看出，只要式（2）中滑模控制率的切换增益$k>cd^*$，系统（1）将在有限时间内驱动到滑模面$s=0$上。令式（2）中$s=0$，可将状态量x_1表示成

$$\frac{\mathrm{d}x_1}{\mathrm{d}t}=-cx_1+d(t)\tag{4}$$

从式（4）中可以看出，即使式（2）中控制率能够使系统状态在有限时间内到达滑模面，系统状态也不能被驱动到期望的平衡点，这就是传统滑模控制方法。

2 基于扰动观测器的滑模控制（DOB-SMC）方法

针对传统SMC方法不能有效的估计外部扰动，现设计一种DOB-SMC方法，设计过程为：令$\boldsymbol{x}=\begin{bmatrix}x_1 & x_2\end{bmatrix}^{\mathrm{T}}$，系统（1）可以表示为

$$\begin{cases}\dfrac{\mathrm{d}\boldsymbol{x}}{\mathrm{d}t}=\boldsymbol{f}(\boldsymbol{x})+\boldsymbol{g}_1(\boldsymbol{x})u+\boldsymbol{g}_2d\\ y=x_1\end{cases}\tag{5}$$

式中，$\boldsymbol{f}(\boldsymbol{x})=\begin{bmatrix}x_2 & a(x)\end{bmatrix}^{\mathrm{T}}$，$\boldsymbol{g}_1(\boldsymbol{x})=\begin{bmatrix}0 & b(x)\end{bmatrix}^{\mathrm{T}}$，$\boldsymbol{g}_2=\begin{bmatrix}1 & 0\end{bmatrix}^{\mathrm{T}}$。设计一个可以估计式（5）中扰动的DOB为[19]

$$\begin{cases}\dfrac{\mathrm{d}p}{\mathrm{d}t}=-\boldsymbol{l}\boldsymbol{g}_2p-\boldsymbol{l}\left[\boldsymbol{g}_2\boldsymbol{l}\boldsymbol{x}+\boldsymbol{f}(\boldsymbol{x})+\boldsymbol{g}_1(\boldsymbol{x})u\right]\\ \hat{d}=p+\boldsymbol{l}\boldsymbol{x}\end{cases}\tag{6}$$

式中，$\hat{d}$，p，$\boldsymbol{l}$分别为外部扰动的估计，DOB的内部状态和待设计的观测器增益。基于式（6）对外部扰动的估计，定义了系统（1）在外部扰动存在下的新滑模面为

$$s = x_2 + cx_1 + \hat{d} \tag{7}$$

式中，c是一个待设计的控制参数。因此，提出基于DOB的滑模控制率为

$$u = -b^{-1}(x)[a(x) + c(x_2 + \hat{d}) + k\mathrm{sgn}(s)] \tag{8}$$

式中，k是符号函数的增益，$\mathrm{sgn}(s)=\begin{cases}1 & s>0\\ -1 & s<0\end{cases}$。对提出的DOB的滑模控制结构框图如图1所示。

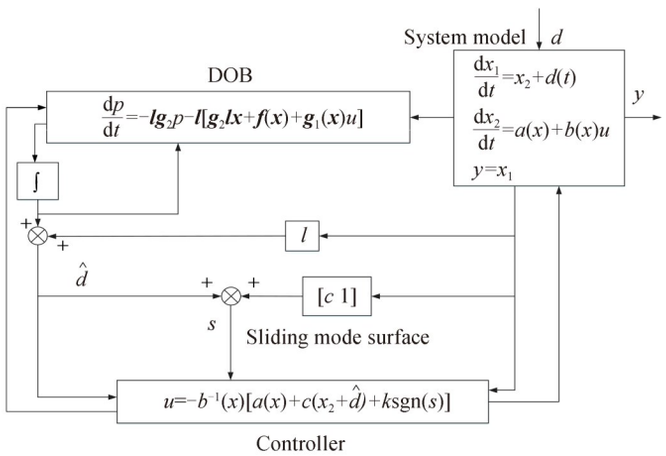

图1　基于DOB的滑模控制结构框图

Fig. 1　Block diagram of sliding mode control structure based on DOB

2.1　DOB-SMC方法稳定性分析

对上述提出的控制方法进行稳定性分析。假设2：系统(1)中外部扰动的导数是有界的，且满足$\lim\limits_{t\to\infty}\dfrac{\mathrm{d}d(t)}{\mathrm{d}t}=0$。如果系统(1)满足假设1和假设2，设计DOB矩阵增益$\boldsymbol{l}$，使$\boldsymbol{lg}_2>0$，则DOB的扰动误差估计可以渐进跟踪系统的误差，那么

$$\frac{\mathrm{d}e_d(t)}{\mathrm{d}t} + \boldsymbol{lg}_2 e_d(t) = 0 \tag{9}$$

是全局渐进稳定的。其中$e_d(t)=d(t)-\hat{d}(t)$是扰动的估计误差。假设3：式(9)中扰动的估计误差有界，定义为$e_d^*(t)=\sup\limits_{t>0}\left|e_d(t)\right|$。

如果系统(1)满足假设1～3，系统在控制率式(8)的前提下，切换增益$k>(c+\boldsymbol{lg}_2)e_d^*$，观测器增益$\boldsymbol{l}$使得$\boldsymbol{lg}_2>0$，则闭环系统渐进稳定。

2.2　DOB-SMC方法验证

对式(7)中定义的滑模面s沿系统(1)进行求导，将控制率式(8)代入可得

$$\frac{\mathrm{d}s}{\mathrm{d}t} = -k\,\mathrm{sgn}(s) + c\left[d(t)-\hat{d}(t)\right] + \frac{\mathrm{d}\hat{d}(t)}{\mathrm{d}t} \tag{10}$$

根据式(6)可以推导出$\dfrac{\mathrm{d}\hat{d}(t)}{\mathrm{d}t}=-\boldsymbol{lg}_2\left[\hat{d}(t)-d(t)\right]$，将其代入式(10)得

$$\frac{\mathrm{d}s}{\mathrm{d}t} = -k\,\mathrm{sgn}(s) + (c+\boldsymbol{lg}_2)e_d(t) \tag{11}$$

选取李雅普诺夫函数为

$$V(s) = 1/2s^2 \tag{12}$$

对式(12)求导，可得

$$\begin{aligned}\frac{\mathrm{d}V}{\mathrm{d}t} &= s\cdot\frac{\mathrm{d}s}{\mathrm{d}t} = -k|s| + (c+\boldsymbol{lg}_2)e_d(t)s\\ &\leqslant -\left[k-(c+\boldsymbol{lg}_2)e_d^*\right]|s| = -\sqrt{2}\left[k-(c+\boldsymbol{lg}_2)e_d^*\right]V^{\frac{1}{2}}\end{aligned} \tag{13}$$

当$k>(c+lg_2)e_d^*$时，根据式(13)可以推导出系统状态将在有限时间内到达滑模面$s=0$上。$s=0$则表示

$$\frac{\mathrm{d}x_1}{\mathrm{d}t}=-cx_1+d(t)-\hat{d}(t) \tag{14}$$

将式(14)与观测器相结合，得

$$\begin{cases}\dfrac{\mathrm{d}x_1}{\mathrm{d}t}=-cx_1+e_d\\ \dfrac{\mathrm{d}e_d}{\mathrm{d}t}=-lg_2e_d+\dfrac{\mathrm{d}d(t)}{\mathrm{d}t}\\ x_2=-cx_1-\hat{d}\end{cases} \tag{15}$$

在给定$c>0$和$lg_2>0$的情况下，验证系统

$$\begin{cases}\dfrac{\mathrm{d}x_1}{\mathrm{d}t}=-cx_1+e_d\\ \dfrac{\mathrm{d}e_d}{\mathrm{d}t}=-lg_2e_d\end{cases} \tag{16}$$

是渐近稳定的。根据这一结果，可推出系统

$$\begin{cases}\dfrac{\mathrm{d}x_1}{\mathrm{d}t}=-cx_1+e_d\\ \dfrac{\mathrm{d}e_d}{\mathrm{d}t}=-lg_2e_d+\dfrac{\mathrm{d}d(t)}{\mathrm{d}t}\end{cases} \tag{17}$$

对于任意有界的外部扰动以及有界的状态初始条件，状态总是有界的，并且当外部扰动为零时，系统总能恢复到平衡点。根据假设2给出的条件，式(17)的状态满足$\lim\limits_{t>0}x_1(t)=0$，$\lim\limits_{t>0}e_d(t)=0$，说明在所提出的控制率下，系统状态将渐近稳定滑动到期望的平衡点。

因此得出结论，为了保证系统稳定性，传统SMC方法和DOB-SMC方法切换增益分别设计为$k>c|d|$，$k>(c+lg_2)\left|d-\hat{d}\right|$。由于DOB对外部扰动进行了精确的估计，因此可以使估计误差$\left|d-\hat{d}\right|$的幅度比扰动的幅度小得多，使其收敛到0。因此，该方法可以在一定程度上缓解抖振问题。

3 仿真实验分析

考虑以下系统进行仿真研究，讨论DOB-SMC方法的可行性，通过MATLAB Simulink搭建倾斜镜控制模型，对比传统SMC方法和DOB-SMC方法的控制效果，控制参数见表1。

$$\begin{cases}\dfrac{\mathrm{d}x_1}{\mathrm{d}t}=x_2+d(t)\\ \dfrac{\mathrm{d}x_2}{\mathrm{d}t}=-2x_1-x_2+u\\ y=x_1\end{cases} \tag{18}$$

表1 控制参数表

Table 1 Control parameter table

Controller	Reference
SMC	$c=4,k=3$
DOB-SMC	$c=4,k=3,l=[5,0]$

对系统分别输入阶跃信号和正弦信号，阶跃信号加入时间为0.1 s，正弦信号幅值为1 mrad，频率为100 Hz，加入幅值为100 μrad的随机信号作为模拟对系统的扰动，阶跃响应扰动信号加入时间为0.1 s，正弦响应扰动信号加入时间为0.01 s。对响应曲线和进入稳态后的误差曲线进行对比，如图2、图3所示。

图2(a)中，与传统SMC方法相比，DOB-SMC方法的动态响应没有出现超调；图2(b)中，采用DOB-

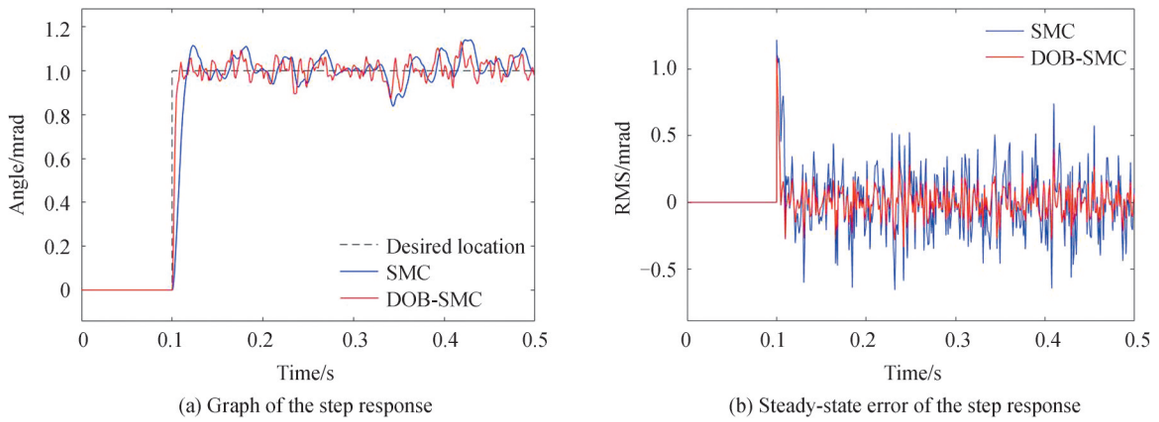

(a) Graph of the step response　(b) Steady-state error of the step response

图2　$c=4$，$k=3$时阶跃信号响应曲线

Fig. 2　Graph of the step signal response of $c=4$, $k=3$

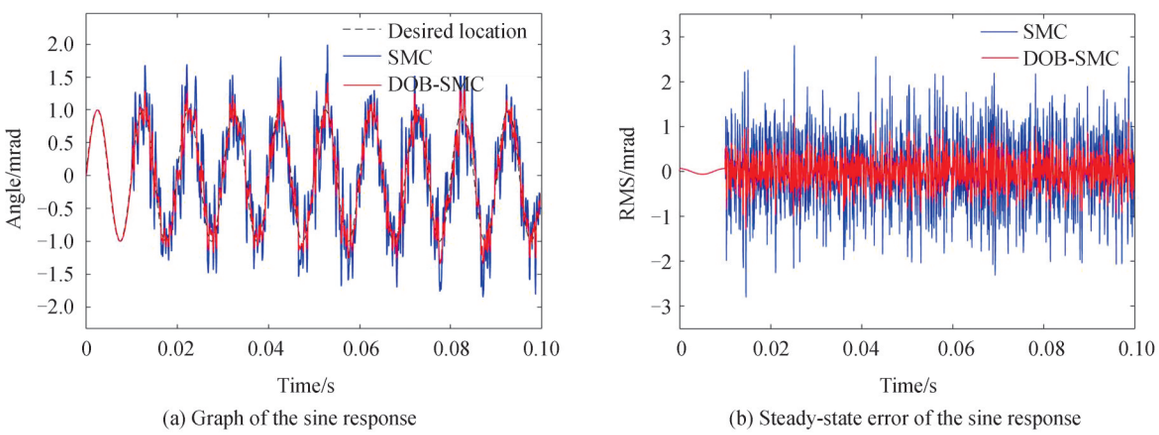

(a) Graph of the sine response　(b) Steady-state error of the sine response

图3　$c=4$，$k=3$时正弦信号响应曲线

Fig. 3　Graph of the sine response of $c=4$, $k=3$

SMC方法抑制扰动效果明显，降低了系统误差。图3中，在没有扰动加入的情况下，传统SMC方法和DOB-SMC方法都能很好的跟踪系统状态，加入扰动后，DOB-SMC方法能够比较准确的跟踪系统状态，输出曲线更接近输入的正弦信号曲线。但是，由于选择了较大的切换增益来抑制扰动，两种方法都产生了很大的抖振。

根据第2节中的结论，通过设置相对较小的切换增益来抑制抖振，控制参数见表2。

表2　控制参数表

Table 2　Control parameter table

Controller	Reference
SMC	$c=4,k=1$
DOB-SMC	$c=4,k=1,l=[5,0]$

将切换增益k从3减小到1，从图4～5中可以看出，提出的DOB-SMC方法可以通过降低切换增益来减小抖振。所提出的DOB-SMC方法在抖振减小的情况下，仍然可以获得良好的控制效果，同时也验证了第2节中的结论。

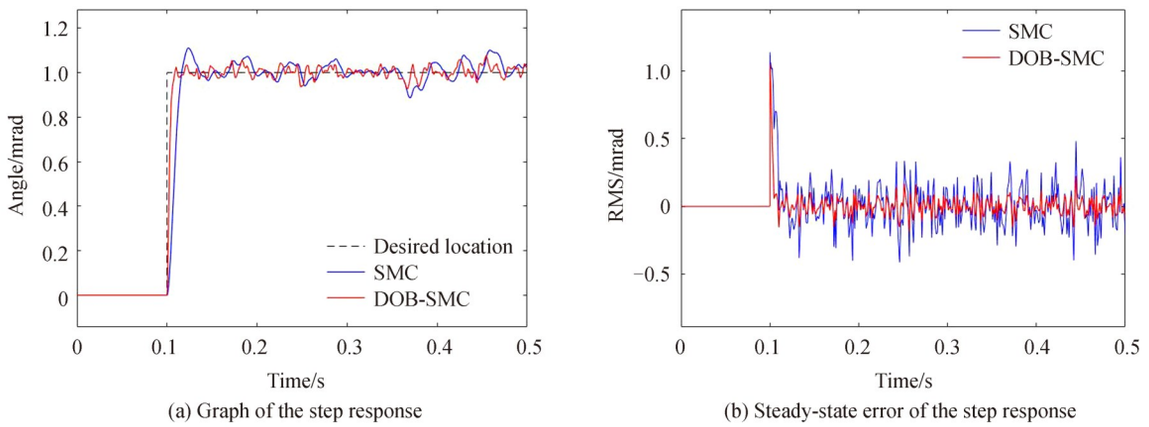

(a) Graph of the step response　(b) Steady-state error of the step response

图 4　c=4，k=1 时阶跃信号响应曲线

Fig. 4　Graph of the step signal response of c=4, k=1

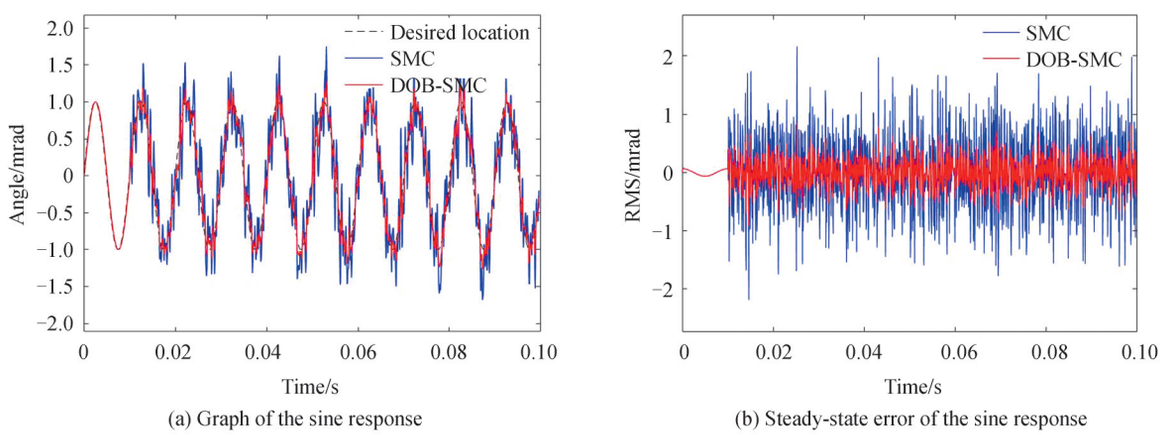

(a) Graph of the sine response　(b) Steady-state error of the sine response

图 5　c=4，k=1 时正弦信号响应曲线

Fig. 5　Graph of the sine response of c=4, k=1

4　实验验证

本文研究外部扰动对自适应光学系统中倾斜镜影响的SMC设计。将自适应光学系统中倾斜镜等效为一个二阶质量-弹簧-阻尼系统，如图 6 所示。

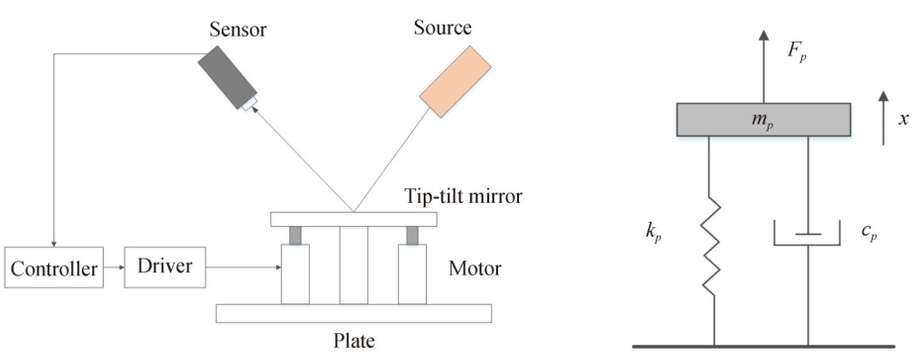

(a) Working principle diagram of the tip-tilt mirror　(b) Structure of the tip-tilt mirror

图 6　倾斜镜系统示意图

Fig. 6　Structure diagram of the tip-tilt mirror system

根据牛顿第二定律可得该系统的动力学模型表示为

$$\begin{cases}\dfrac{\mathrm{d}x}{\mathrm{d}t}=\boldsymbol{A}x+\boldsymbol{B}_u u+\boldsymbol{B}_d d\\ y=\boldsymbol{C}x\end{cases}\tag{19}$$

式中，系统状态分别为倾斜镜位置x_1，响应速度x_2和系统的外部扰动d，$\boldsymbol{x}=\begin{bmatrix}x_1 & x_2\end{bmatrix}^{\mathrm{T}}$，$\boldsymbol{A}=\begin{bmatrix}0 & 1\\ -\dfrac{1}{m_p}\left(k_p+\dfrac{T_{\mathrm{em}}^2}{C_p}\right) & -\dfrac{c_p}{m_p}\end{bmatrix}$，$\boldsymbol{B}_u=\begin{bmatrix}0\\ \dfrac{T_{\mathrm{em}}}{m_p}\end{bmatrix}$，$\boldsymbol{B}_d=\begin{bmatrix}1\\0\end{bmatrix}$，$\boldsymbol{C}=\begin{bmatrix}1 & 0\end{bmatrix}$，倾斜镜系统参数见表3。

表3　倾斜镜系统参数表

Table 3　System parameters of the tip-tilt mirror

Parameter	Meaning	Reference
m_p	Equivalent mass	200 g
c_p	Equivalent damping	35 N•s/m
k_p	Equivalent stiffness	18 N/μm
C_p	Equivalent capacitance	3.6 μF
T_{em}	Electromechanical ratio	0.51

将DOB、滑模面和控制率分别设计为

$$\begin{cases}\dfrac{\mathrm{d}p}{\mathrm{d}t}=-\boldsymbol{L}\boldsymbol{B}_d p-\boldsymbol{L}\left[\boldsymbol{B}_d\boldsymbol{L}\boldsymbol{x}+\boldsymbol{A}\boldsymbol{x}+\boldsymbol{B}_u u\right]\\ \hat{d}=p+\boldsymbol{L}\boldsymbol{x}\end{cases}\tag{20}$$

$$s=c_1x_1+c_2(x_2+\hat{d})\tag{21}$$

$$u=-\boldsymbol{B}_u^{+}\left[\boldsymbol{A}\boldsymbol{x}+\boldsymbol{B}_d\hat{d}+c_2(x_2+\hat{d})+k\,\mathrm{sgn}(s)\right]\tag{22}$$

式中，c_1，c_2必须满足Hurwitz矩阵，即$P_0(z)=c_2z+c_1=0$，系统渐近稳定。$\boldsymbol{B}_u^{+}$为$\boldsymbol{B}_u$的广义逆矩阵。对式(21)中滑模面求导，得

$$\frac{\mathrm{d}s}{\mathrm{d}t}=-k\,\mathrm{sgn}(s)+\left[c_1+c_2\boldsymbol{L}\boldsymbol{B}_d\right]e_d(t)\tag{23}$$

令$k>(c_1+c_2\boldsymbol{L}\boldsymbol{B}_d)e_d^{*}$，所提出的控制率能够保证系统的滑模运动，即系统在滑动模面上的状态能渐进移动到平衡点。控制参数见表4。

表4　倾斜镜控制参数表

Table 4　Control parameters of the tip-tilt mirror

Controller	Reference
SMC	$c_1=80$，$c_2=15$，$k=15$
DOB-SMC	$c_1=80$，$c_2=15$，$k=15$，$L=[120,0]$

对传统SMC方法和DOB-SMC方法进行对比，在误差满足小于5 μrad的情况下，搭建了实验系统如图7所示，在室内环境下进行了倾斜镜对模拟大气湍流的倾斜校正测试。实验装置分为两部分组成，发射部分和接收部分。发射装置作为模拟目标源，经过模拟大气湍流后到达倾斜镜系统，其由激光器和平行光管组成。接收装置为光端机的控制系统，由倾斜镜、变形镜、哈特曼传感器、CCD相机、精跟踪伺服系统及上位机系统组成。

发射装置的信标光和通信光是同轴发射，其中采用波长为785 nm的激光器作为信标光源，波长为1 530 nm的激光器作为通信光源。倾斜镜选用芯明天P32系列压电偏转镜，口径25 mm，方位轴和俯仰轴最大偏转角度为6 mrad，最小偏转分辨率为0.1 μrad；变形镜采用21单元变形镜，口径35 mm；哈特曼传感器子孔径为7×7，单个子孔径占10×10个像元。激光经10 m平行光管整形后出射，光束经倾斜镜校正后入射至变形镜。CCD相机的帧频设置为100 Hz，脱靶量信息从相机中获得，像元角分辨率为5 μrad/pixel，将相邻两帧

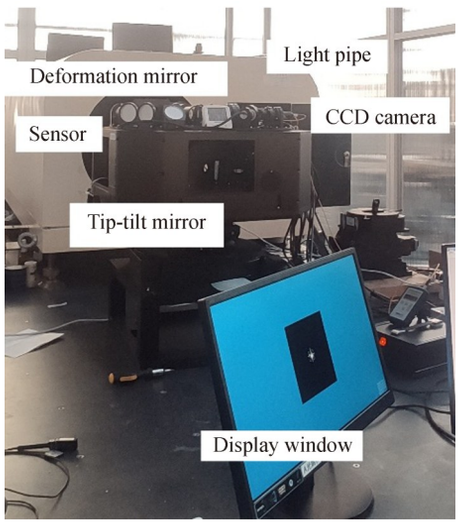

图 7 实验装置图

Fig. 7 Experimental device diagram

间的脱靶量转换为微弧度,得到差值,在上位机上计算并显示均方根值。倾斜镜方位轴和俯仰轴实时校正结果如图 8~9 所示,位置误差结果如图 10~11 所示。

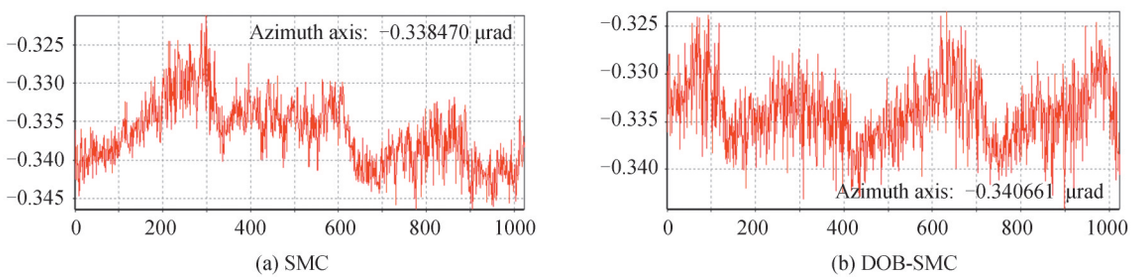

图 8 倾斜镜方位轴校正曲线

Fig. 8 Azimuth axis calibration curve of the tip-tilt mirror

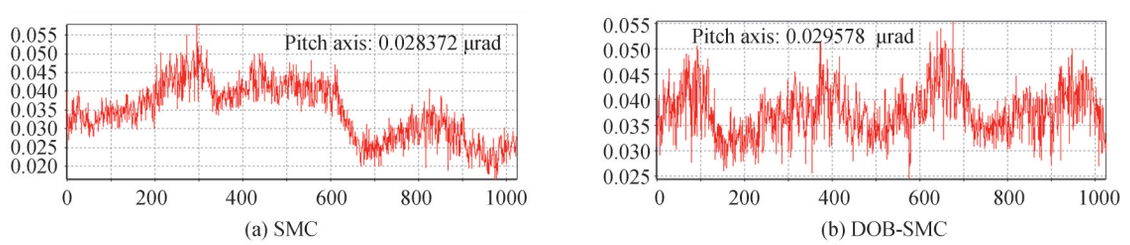

图 9 倾斜镜俯仰轴校正曲线

Fig. 9 Pitch axis calibration curve of the tip-tilt mirror

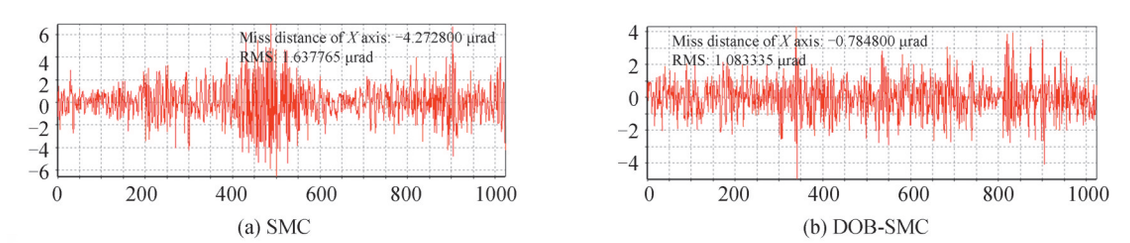

图 10 倾斜镜方位轴校正误差曲线

Fig. 10 Azimuth axis correction error curve of the tip-tilt mirror

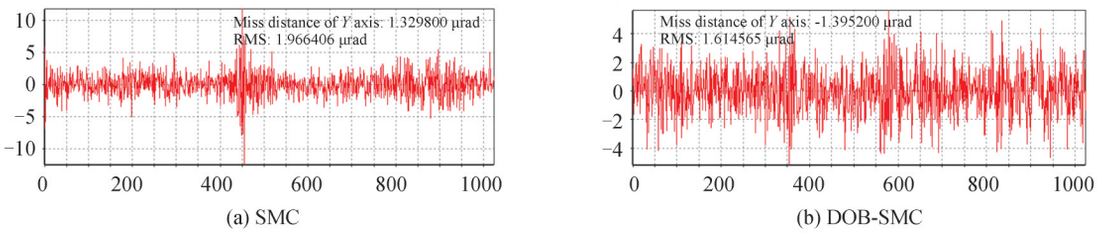

图 11　倾斜镜俯仰轴校正误差曲线

Fig. 11　Pitch axis correction error curve of the tip-tilt mirror

图 8～9 中，采集的数值为倾斜镜方位轴和俯仰轴的校正实时值，与传统 SMC 方法相比，DOB-SMC 方法校正曲线较平稳，实时校正误差可以根据图 10～11 对比看出，在相机视场中，X 脱靶量对应倾斜镜方位轴，Y 脱靶量对应倾斜镜俯仰轴，将采集到的脱靶量数据计算出均方根值，对比两轴的校正误差。DOB-SMC 方法的控制性能要优于传统 SMC 方法，抑制扰动幅度较小，在采用传统 SMC 方法时，方位轴的误差均方根值（Root Mean Square，RMS）为 1.64 μrad，俯仰轴的误差 RMS 为 1.97 μrad，采用 DOB-SMC 方法时，方位轴的误差 RMS 为 1.08 μrad，俯仰轴的误差 RMS 为 1.61 μrad。该控制策略下，控制反馈精度优于 5 μrad，整体性能相较于传统 SMC 大大提高。

5　结论

针对倾斜镜抑制外部扰动的控制问题，提出了一种基于扰动观测器的滑模控制方法来减小误差，设计了一种新的滑模面，该滑模面包含了扰动估计，在不确定扰动的情况下，沿滑模面的滑模运动可以将系统状态驱动到期望的平衡点。该方法在没有扰动存在的情况下可以与传统滑模控制相同，但是在系统状态发生变化的时候会抑制抖振。仿真和实验都验证了该方法的有效性和优越性。实验结果表明，倾斜镜方位轴误差 RMS 为 1.08 μrad，与传统 SMC 方法相比，控制精度提高约 51.2%，俯仰轴误差 RMS 为 1.61 μrad，与传统 SMC 方法相比，控制精度提高约 21.8%，保证了倾斜镜的波前探测精度。由于室内实验时扰动对系统影响较小，保留了 3 μrad 的提升表现，为后续室外实验留有余量。

参考文献

[1] ZHANG Jiaheng. Modeling and control of a fast steering mirror system for wireless laser communication in marine environment [D]. Hangzhou: Zhejiang University, 2017.
张嘉恒. 用于海洋环境无线激光通信的倾斜镜系统建模及控制方法研究[D]. 杭州：浙江大学, 2017.

[2] WANG Yukun, HU Lifa, WANG Chongchong, et al. Modeling and control of Tip/Tilt mirror in liquid crystal adaptive optical system[J]. Optics and Precision Engineering, 2016, 24(4): 771-779.
王玉坤，胡立发，王冲冲，等. 液晶自适应光学系统中倾斜镜的建模与控制[J]. 光学精密工程, 2016, 24(4): 771-779.

[3] WANG Yukun. Research on the control of adaptive optical system for space laser communication [D]. Changchun: Changchun Institute of Optics, Fine Mechanics and Physics, Chinese Academy of Sciences, 2019.
王玉坤. 空间激光通信自适应光学系统的控制研究[D]. 长春：中国科学院长春光学精密机械与物理研究所, 2019.

[4] CORREIA C, VÉRAN J P, HERRIOT G. Advanced vibration suppression algorithms in adaptive optics systems. [J]. Journal of the Optical Society of America A, 2012, 29(3): 185-194.

[5] PETIT C, CONAN J M, KULCSÁR C, et al. First laboratory validation of vibration filtering with LQG control law for adaptive optics[J]. Optics Express, 2008, 16(1): 87-97.

[6] CASTRO M, ESCÁRATE P, GARCÉS J, et al. Closed-loop control for tip-tilt compensation on systems under vibration [C]. Adaptive Optics Systems V. International Society for Optics and Photonics, 2016, 9909: 99093K.

[7] KECK A, POTT J U, SAWODNY O. Accelerometer-based online reconstruction of vibrations in extremely large telescopes[J]. IFAC Proceedings Volumes, 2014, 47(3): 7467-7473.

[8] BÖHM M, POTT J U, KÜRSTER M, et al. Delay compensation for real time disturbance estimation at extremely large telescopes[J]. IEEE Transactions on Control Systems Technology, 2016, 25(4): 1384-1393.

[9] GLÜCK M, POTT J U, SAWODNY O. Piezo-actuated vibration disturbance mirror for investigating accelerometer-based tip-tilt reconstruction in large telescopes[J]. IFAC-PapersOnLine, 2016, 49(21): 361-366.

[10] PETIT C, CONAN J M, KULCSÁR C, et al. Linear quadratic Gaussian control for adaptive optics and multiconjugate adaptive optics: experimental and numerical analysis[J]. Journal of the Optical Society of America A, 2009, 26(6): 1307-

1325.
[11] GUESALAGA A, NEICHEL B, O'NEAL J, et al. Mitigation of vibrations in adaptive optics by minimization of closed-loop residuals[J]. Optics Express, 2013, 21(9): 10676-10696.
[12] KEMPF C J, KOBAYASHI S. Disturbance observer and feedforward design for a high-speed direct-drive positioning table[J]. IEEE Transactions on control systems Technology, 1999, 7(5): 513-526.
[13] ZHENG M, ZHOU S, TOMIZUKA M. A design methodology for disturbance observer with application to precision motion control: an H-infinity based approach[C]. 2017 American Control Conference (ACC), IEEE, 2017: 3524-3529.
[14] YANG J, LI S, YU X. Sliding-mode control for systems with mismatched uncertainties via a disturbance observer[J]. IEEE Transactions on Industrial Electronics, 2012, 60(1): 160-169.
[15] TOMIZUKA M. Controller structure for robust high-speed/high-accuracy digital motion control[C]. Tutorial of 1994 IEEE International Conference on Robotics and Automation, 1994.
[16] YAO B, AL-MAJED M, TOMIZUKA M. High-performance robust motion control of machine tools: an adaptive robust control approach and comparative experiments[J]. IEEE/ASME Transactions on Mechatronics, 1997, 2(2): 63-76.
[17] LIU H X, LI S H. Speed control for PMSM servo system using predictive functional control and extended state observer [J]. IEEE Transactions on Industrial Electronics, 2011, 59(2): 1171-1183.
[18] CHEN W H. Nonlinear disturbance observer-enhanced dynamic inversion control of missiles[J]. Journal of Guidance, Control, and Dynamics, 2003, 26(1): 161-166.
[19] YANG Chengshun, HUA Tao, DAI Yuchen, et al. Wide speed domain anti-interference sliding mode control of permanent magnet synchronous motor for electric vehicle [J]. Electric Machines & Control Application, 2021, 48(12): 21-29.
杨成顺,华涛,戴宇辰,等.电动汽车用永磁同步电机宽速域抗干扰滑模控制[J].电机与控制应用, 2021, 48(12): 21-29.

Sliding Mode Control of Tip-tilt Mirror Based on Disturbance Observer

ZHAO Dechun[1], SONG Yansong[2,3], LIU Yang[2,3], DONG Yan[1,2], ZHANG Baishuo[3]
(1 *School of Electronic Information Engineering, Changchun University of Science and Tecnology, Changchun* 130022, *China*)
(2 *Fundamental Science on Space-Ground Laser Communication Technology Laboratory, Changchun University of Scienceand Technology, Changchun* 130022, *China*)
(3 *School of Optoelectronic Engineering, Changchun University of Science and Technology, Changchun* 130022, *China*)

Abstract: Tip-tilt mirror is a type of precision optical equipment that controls the direction of beam propagation in modern photoelectric systems. It has been utilized in space laser communications, adaptive optics, vehicle/airborne laser systems, image stabilization, astronomical telescopes, confocal microscopy, real-time laser scanning, capture target tracking, and other applications. The tip-tilt mirror is used in adaptive optics to correct the phase wavefront caused by atmospheric turbulence, which accounts for approximately 87% of the overall tilt. As a result, the tip-tilt mirror helps to rectify the first-order tilt of the system. The closed-loop performance of the adaptive optics system is severely harmed because the tip-tilt mirror is susceptible to wind vibration, equipment vibration, and platform vibration. As a result, the vibration must be minimized to approach the diffraction limit of optics. The standard closed-loop feedback control is ineffective in suppressing the vibration of the tip-tilt mirror, reducing closed-loop performance. In consequence, research into novel anti-vibration technology is critical to improving the closed-loop performance of the tip-tilt mirror. There are numerous methods for reducing vibration in use today. For example, literature offered a disturbance-based feedforward control method to suppress structural vibration of the tip-tilt mirror system, which involved measuring the disturbance with an accelerometer or a gyroscope and then feeding the disturbance with signal reconstruction. Returning to the system, the controller is not limited by low-rate sampling because it can produce a large suppression bandwidth. Additional measurement equipment, on the other hand, will raise the cost of the system as well as its complexity and analytical difficulty. Accelerometers or gyroscopes suffer from severe low-frequency drift and high-frequency noise. Existing control systems face extra control issues as a result of the accuracy of

vibration estimation. Many enhanced control structures and optimized controllers, such as the Linear Quadratic Gaussian controller (LQG) and H_∞/H_2controller, have been developed based on the assumption of perturbation feedforward control. The results demonstrate that these strategies can improve the closed-loop performance of the system by 20% to 30%. However, the performance of the closed-loop system is dependent on the model accuracy and vibration of the controlled object. For example, in the tip-tilt mirror control system, if the model error is considerable, the performance of the system would be severely hampered. Because interference normally occurs in the low-frequency domain while sensor noise occurs in the high-frequency domain, a disturbance observer is employed to suppress interference in the low-frequency domain when the interference can be reliably estimated or measured. The Q-filter is commonly employed as an optimum filter in various servo control systems to maximize closed-loop performance in terms of control bandwidth and robust stability. When low-frequency and intermediate-frequency interference are significant, the high bandwidth of the low-pass filter is necessary. Sliding Mode Control (SMC) is widely used in industry because of its simple algorithm, strong anti-interference ability, and ability to overcome system uncertainty. However, the uncertainty existing in many practical systems does not satisfy the matching conditions of the system. For example permanent magnet synchronous motor system due to uncertainty caused by parameter variation and load torque, flight control system without dynamic modeling, external wind vibration, and parameter variation causing concentrated disturbance torque, For these systems, the sliding-mode motion of conventional SMC suffers from mismatch perturbations, which greatly reduces their robustness.To solve the control problem of the tip-tilt mirror in Adaptive Optics with the external disturbance, a disturbance observer was designed based on the sliding mode control (DOB-SMC) to suppress structural vibration. A new disturbance observer (DOB) was added to the traditional SMC method in the tip-tilt mirror control system, and a new sliding mode control rate was designed to suppress chattering. The improved DOB was not limited by precise models. And the emulation proved that this method is achievable. The experimental results showed that the control error of the azimuth axis is reduced from 1.637 μrad to 1.083 μrad, and the accuracy is improved by about 51.2%. The control error of the pitch axis is reduced from 1.966 μrad to 1.614 μrad, and the accuracy is improved by about 21.8%. This method can greatly weaken the inherent chattering and external disturbance of the system, and improve the stability of the tip-tilt mirror system.

Key words: Adaptive optics; Tip-tilt mirror; Sliding mode control; Disturbance observer; Chattering

OCIS Codes: 010.1080; 250.0250; 250.3140

Foundation item: Natural Science Foundation of Science and Technology Department of Jilin Province (No. YDZJ202101ZYTS193)